

Supersonic Flow past a Blunt Cone under the Action of Plasma Formation

Irina Znamenskaya^{1*}, Vladimir Chernikov¹, Olga Azarova², Dmitry Naumov¹

¹Lomonosov Moscow State University, Russia, Moscow, 119234, Leninskie Gory 1, build. 2

²Dorodnicyn Computing Centre, Federal Research Center "Computer Science and Control" of RAS
Russia, Moscow, 119333, Vavilova str. 40

Abstract

Experimental and CFD analysis of plasma formation impact on the supersonic flow (M=3) around a body "blunt cone - cylinder" is presented. Special attention is drawn to bow-blast waves interaction visualized with high speed shadowgraphy. Calculations are based on Euler equations. The plasmoid is modeled by instant energy deposition to a bounded volume, the pressure there being much higher than the pressure in the surrounding gas. Such an explosive process generates a divergent shock wave and affects the bow shock area which becomes the main factor reducing the drag force. Qualitative agreement of CFD patterns with the experiment was obtained.

1. Nomenclature

M	=	freestream Mach number
γ	=	ratio of specific heats
$p_\infty, \rho_\infty, u_\infty, v_\infty$	=	freestream pressure, density and velocity components
D	=	diameter of a cylinder part of AD body
D_f	=	diameter of a frontal surface of AD body
D_i	=	distance from a cylinder part and a frontal surface of AD body
t_i	=	time moment of an energy source arising
p_i	=	pressure in an energy source
r_i	=	radius of an energy source
x_0	=	distance between the center of an energy source and a frontal surface of AD body

AD Aerodynamic

MW Microwave

2. Introduction

Control of supersonic flows by means of plasma formations generated by electrical discharges, microwave energy deposition and laser pulses is currently an extensive area of aerospace engineering [1, 2]. Reorganization of unsteady flow under the action of an external energy deposition was firstly researched in [3, 4] for supersonic streamlining a blunt body. In air the effect of the external energy source produced by MW discharge was shown to lead to the decrease in the stagnation pressure together with the reduction of a drag force of a blunt cylinder [5]. Vortex mechanism of these phenomena was established. MW energy deposition effects on a supersonic flow over cylinder bodies were studied experimentally in [6, 7] and numerically in [8]. Experimental results on laser impulse impact were presented in [9-11] and were numerically analysed in [12, 13]. Discharge plasma effect was investigated experimentally in [14]. Essential impact on dynamics of the frontal drag force and the bow shock of the action of a heated area produced by energy deposition was obtained in all these studies. In experiments the possibility of using plasma formations (plasmoids) to change the supersonic flow near the model has been investigated in [15].

This paper is devoted to the experimental and numerical research of the plasmoid effect on the shock structure and frontal drag force during the supersonic streamlining a body "blunt cone - cylinder". Comparison of the experimental

*znamen@phys.msu.ru

Shlieren images and computation flow patterns is analysed together with the frontal surface drag force dynamics and the dynamics of fronts of shock waves in the developing shock-wave structures.

3. Experimental study

3.1 Experimental setup

Setup is the combination Laval nozzle which had been designed for Mach number $M = 2-3.5$ and a plasma generator. It is based on a magnetoplasma compressor. These devices are mounted in low-pressure chamber (1 on Fig.1). High pressure at the nozzle inlet was varied from 0.2 to 0.5 from that of the magnetoplasma compressor. The pressure at the nozzle inlet was supplied by a valve via connecting pile 3. Power was supplied to the compressor via connector 4. When a high-voltage pulse was fed to spark gap 6, the supply voltage was fed to the magnetoplasma compressor, and it was discharged with generation of a plasma jet. Electric current time duration $\sim 100 \mu\text{s}$, maximal current $\sim 12 \text{ kA}$, and voltage drop across the discharge 700V ; average electron density $10^{15} - 10^{16} \text{ cm}^{-3}$. Freestream Mach number tested was 3. Diameter of a cylinder part of the body $D = 1.6 \cdot 10^{-2} \text{ m}$; diameter of a frontal surface of the body $D_f = 9 \cdot 10^{-3} \text{ m}$.

Classical Tepler shadow scheme was used including parallel light beam. Digital recording system with high temporal and spatial resolutions was used. High-speed digital camera has the exposure time of a frame about $1 \mu\text{s}$. Recording regimes with 150000 frame/s and 325000 frame/s were used; the interval between frames was about 7 and $4 \mu\text{s}$, respectively. The films of duration up to 3 s including all stages of the gasdynamic process have been recorded.

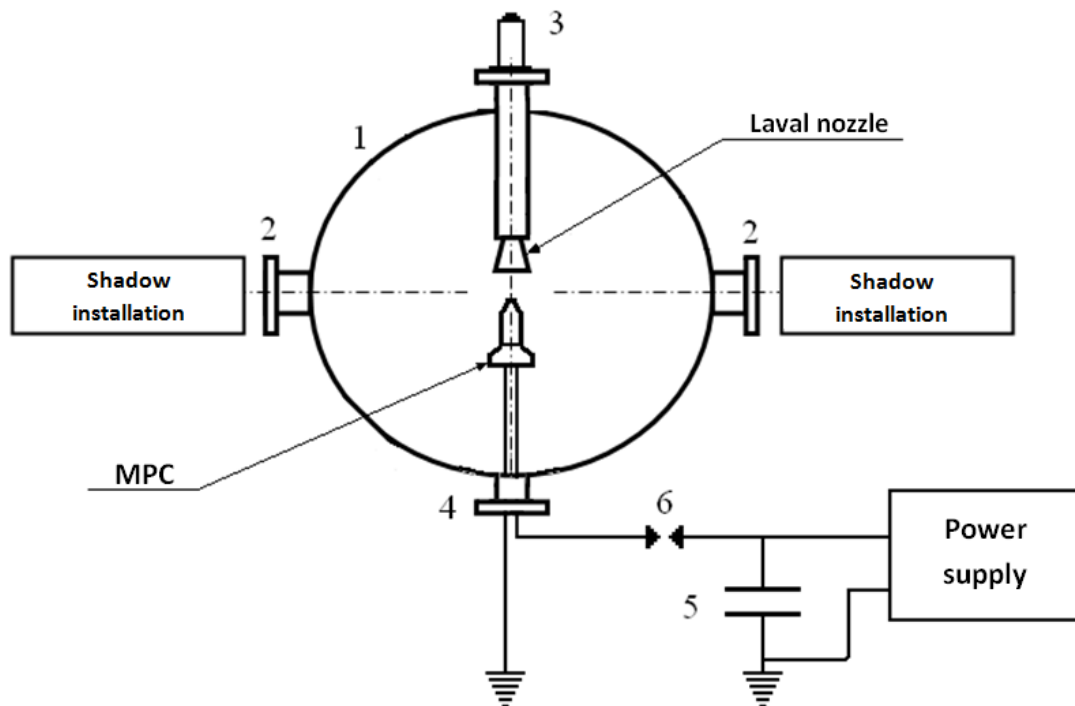
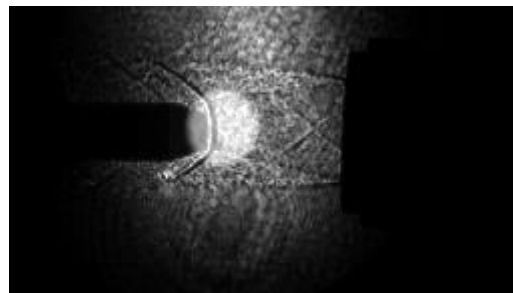


Figure 1: Experimental installation (schematic)

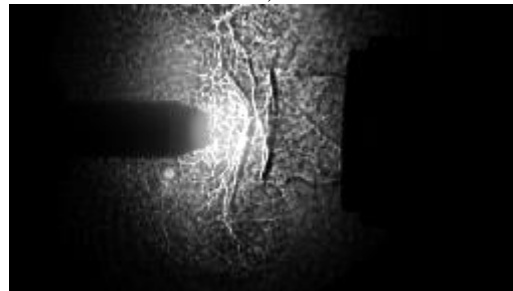
3.2 Experimental results

High speed shadow imaging showed that due to the short time of plasma energy release a blast wave arises. Its dynamics controls the non-steady stage of a new shock-wave structure evolution. In front of the streamlined body the shock layer was shown to reconstruct and the value of the bow shock wave standoff on the axis of symmetry increases significantly – approximately by the value of the plasmoid diameter (4 cm). This indicates a decrease in the flow local Mach number, predominantly due to the sound velocity increase in the plasma region. It should be accompanied by the drag force decrease. Shlieren images of the plasmoid impact on the supersonic flow are presented in Fig. 2. Steady state is established up to 140-170 μ s; some fracture of the bow shock wave is due to the method of organizing a supersonic flow by means of a nozzle.

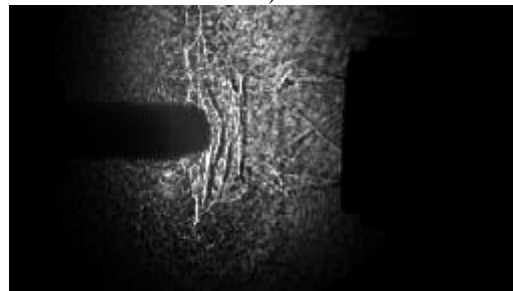
After the steady state establishing the energy deposition begins (Fig. 2a) causing a strong reconstruction of the whole flow. In the experiment the time instant of the discharge inclusion is accepted as the initial time. It is seen the shock structures consisting of several shock waves (Figs. 2b, 2c) which interact with each other (Figs. 2d, 2e) and finally form a new bow shock when the flow becomes steady again after the end of the impact of an energy deposition (Fig. 2f).



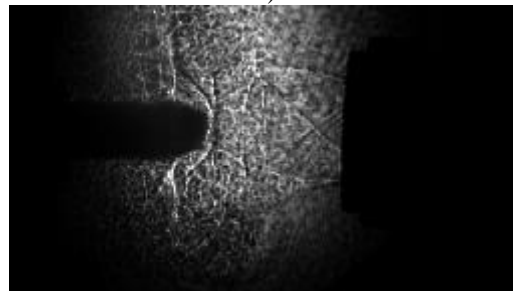
a)



b)



c)



d)

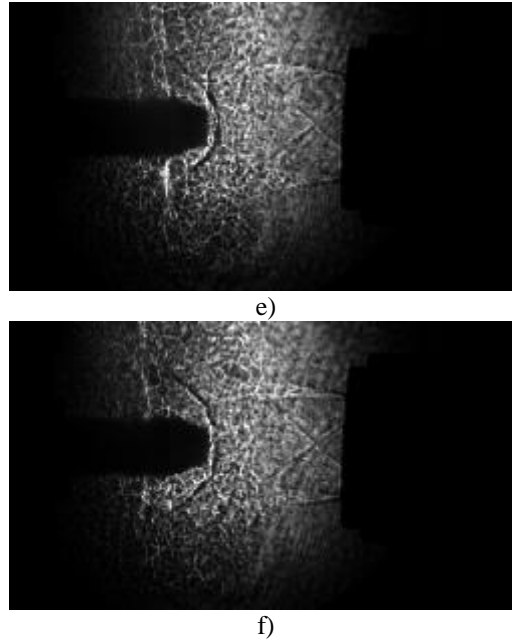


Figure 2 : Shlieren images: a) $t=0$; b) $t=107\mu\text{s}$; c) $t=140\mu\text{s}$; d) $t=166\mu\text{s}$; e) $t=173\mu\text{s}$; f) $t=193\mu\text{s}$

3. Numerical simulations

3.1 Methodology

Supersonic flow over AD body “blunt cone - cylinder” under the impact of an energy deposition is studied at $M=3.1$. The simulations are based on the Euler system of equations for perfect inviscid gas with the ratio of specific heats $\gamma=1.4$:

$$(\mathbf{U}r)_t + (\mathbf{F}r)_x + (\mathbf{G}r)_r = \mathbf{H}, \quad (1)$$

$$\mathbf{U} = (\rho, \rho u, \rho v, E)^T, \mathbf{F} = (\rho u, p + \rho u^2, \rho uv, u(E + p))^T,$$

$$\mathbf{G} = (\rho v, \rho uv, p + \rho v^2, v(E + p))^T, \mathbf{H} = (0, 0, p, 0)^T,$$

$$E = \rho(\varepsilon + 0.5(u^2 + v^2)).$$

The state equation for a perfect gas is used:

$$\varepsilon = p/(\rho(\gamma - 1)).$$

Here ρ , p , u , v are the gas density, pressure and velocity x - and y -components, ε is the specific internal energy. Initial conditions for the problem are the fields of gas parameters in a converged supersonic steady flow past the body (Fig.3).

Energy source is supposed to have a spherical shape. It is assumed to arise instantly in the steady flow at the time moment t_i , the coordinate of its center x_0 is chosen from the experiment. The radius of the energy source is chosen so that the volume to be located in front of the bow shock wave. Pressure in the energy source p_i is supposed to be larger than in the surrounding flow and density and velocity are the same (so the temperature in the energy source is increased in comparison with the surrounding flow). So the model of the instant explosion of a bounded gas volume is used for the energy deposition. The pressure value p_i in the energy source is defined from the relation :

$$\eta E_0 = 4/3\pi r_i^3 (p_i - p_\infty) / (\gamma - 1).$$

Here η is the part of the discharge energy spent to the expansion of a gas, $E_0=500\text{J}$ (from the experiment). In the simulations η was set to 0.07, i.e. it was supposed that 7% of the energy was spent for the gas expansion.

The problem is solved in the dimensionless variables. Dimensionless quantities for time, spatial variables, components of sound velocity and velocity, gas density, pressure and temperature are expressed through the dimensional ones (marked with index “dim”) as follows:

$$t = t_{\text{dim}} / t_n, x = x_{\text{dim}} / l_n, r = r_{\text{dim}} / l_n, u = u_{\text{dim}} / u_n, v = v_{\text{dim}} / v_n, c = c_{\text{dim}} / v_n, \\ \rho = \rho_{\text{dim}} / \rho_n, p = p_{\text{dim}} / p_n, T = T_{\text{dim}} / T_n.$$

Here the following scales for the parameters are accepted:

$$\rho_n = \rho_\infty, p_n = p_\infty, l_n = k_l^{-1} D, T_n = T_\infty, u_n = (p_\infty / \rho_\infty)^{0.5}, t_n = l_n / u_n,$$

where k_l is the dimensionless value of D . Complex conservative difference scheme of the second approximation order in space and in time is used in the calculations [16]. The body’s boundaries are introduced into the calculation area without breaking conservation properties in it. The staggered numerical grid in the calculation area (selected taking into account the symmetry of the flow) contains 10^6 working nodes and about 10^3 nodes are dislocated on the diameter of a cylinder part of the body D .

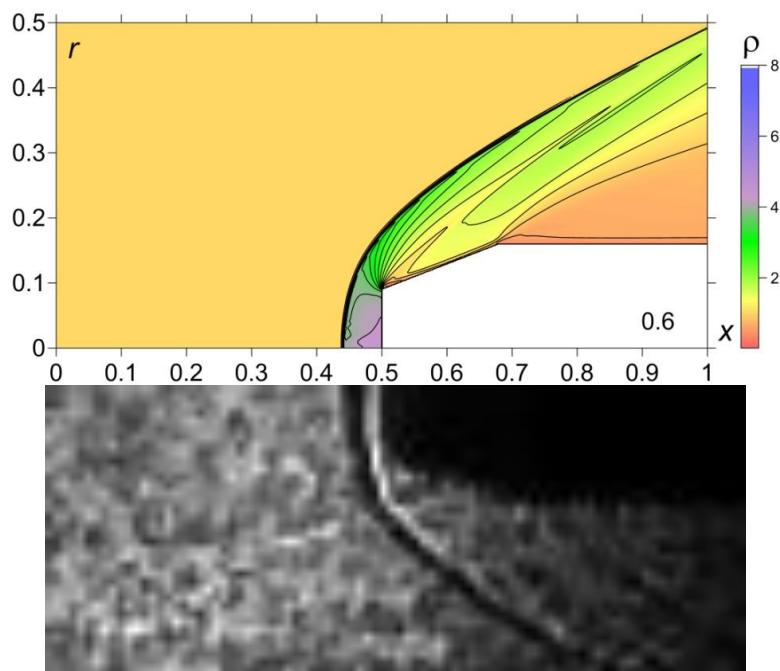


Figure 3 : Steady flow: comparison with the experiment, *upper* – calculations, *bottom* – experiment (enlarged and rotated)

4. Results and discussion

The interaction of the energy source with the shock layer was shown to provide the reorganisation of the whole flow. The gas in the is energy source moves from its center to the periphery and moves towards the bow shock as well. So the shape of the energy source becomes asymmetrical. The process of the instant explosion is accompanied by the break of a shock on the boundary of the compressed gas which can be described in 1D approach by the solution of the Riemann problem of decay of an arbitrary discontinuity. As a result of the gas expansion the shock wave and contact discontinuity radiating from the center are originated and a rarefaction wave moving to the volume center. For a particular set of the parameters a weak shock wave also can be generated from a boundary of the rarefaction wave. By this way an area of the heated gas is formed in the internal part of a region of the expansion gas. The impact of this area was shown to become a reason of front drag force reduction under the action of energy deposition [12, 13].

In Fig. 4 the initial stage of dynamics of energy source-shock layer interaction is presented (dimensionless time moments are shown in the right bottom angle). At the beginning of the interaction ($t=0.6053$) a strong shock wave structure is formed which is caused by the source shock wave and contact discontinuity interaction with the bow shock ($t=0.62$). The bow shock diffraction is seen during the interaction with the formation of a triple configuration. The changing bow shock is seen in the area between the source shock wave and the contact discontinuity, it is

weakened inside the heated central area and becomes almost invisible ($t=0.66$). Later it comes to the less hot left area between the contact discontinuity and the source shock wave and is strengthened there ($t=0.7$).

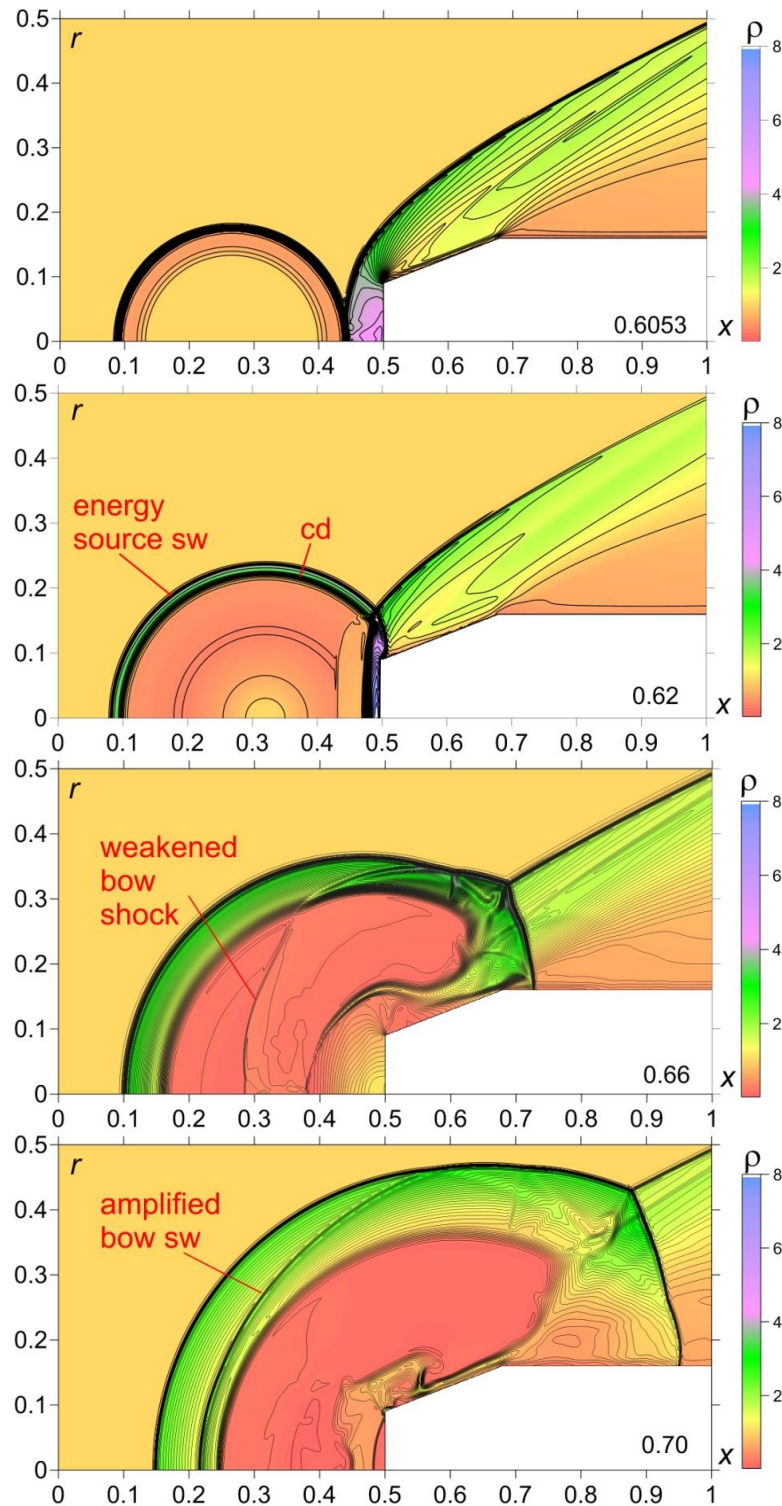


Figure 4: Initial stage of dynamics of energy source-shock layer interaction

In Fig. 5 the middle stage of the interaction is presented. The bow shock is weakened again ($t=0.76$) and later it merges with the source shock wave. At the same time a new shock wave is formed at the heated area boundary. This shock wave formation can be explained by the interaction of the reflected weak shock wave (which is mentioned in Part 3.1) with the contact discontinuity. During the moving of the perturbation area to the body a series of the shock

waves is generated near the front surface of the body ($t=0.8165 - 0.86$). They merge together originating a strong shock wave which interacts with the left part of the source wave forming a new bow shock ($t=0.88$).

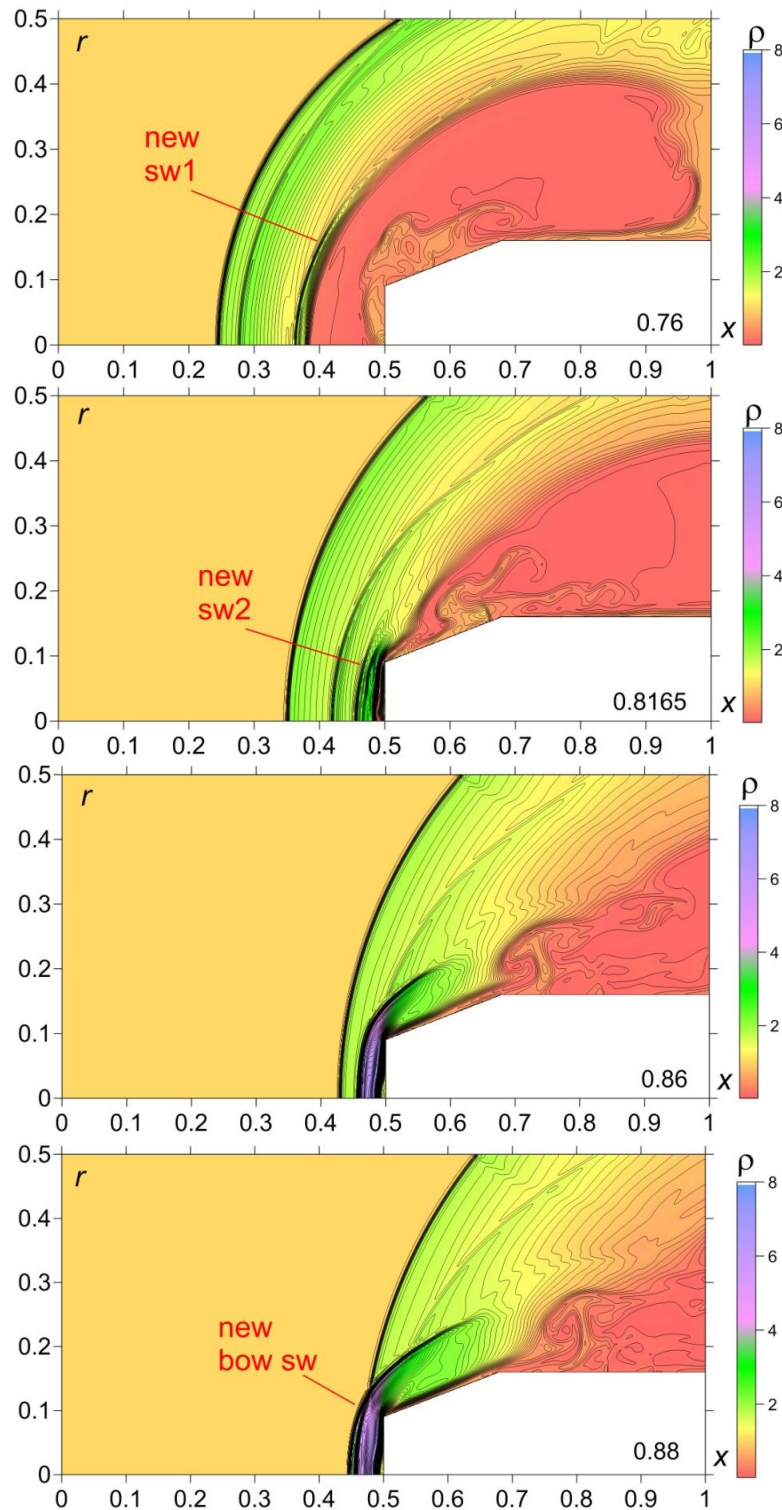


Figure 5: Middle stage of dynamics of energy source-shock layer interaction

Fig. 6 demonstrates the final stage of the interaction. The new bow shock is moving to the left accompanied by the another shock which is the rest part of the source shock wave ($t=0.9-0.94$). Then it stops and begins to move to the body ($t=0.94-0.98$). Finally the flow returns to the initial steady state ($t=1.2$). Trajectories of the obtained shocks are presented in Fig. 7.

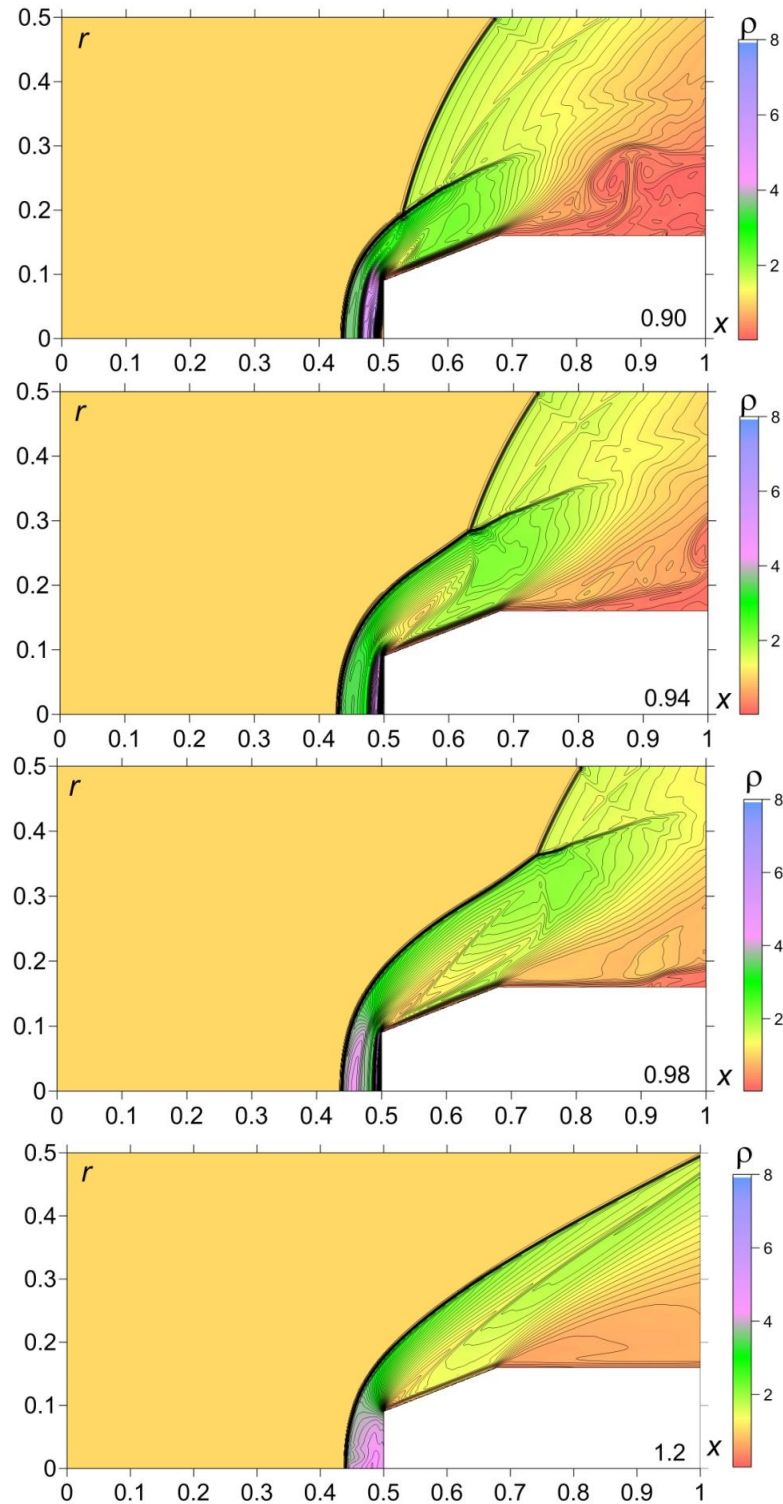


Figure 6: Final stage of dynamics of energy source-shock layer interaction

The impact of the energy deposition is a reason of the essential front drag force reduction which is taken place simultaneously with the moving of the bow shock from the AD body. Fig. 8 shows the dynamics of the stagnation pressure for two values of pressure in the energy source. It is seen that for achieving continuous in time drag reduction the significantly great pressure values in the energy source are needed.

It should be noted that the simulations on the base of the Euler system of equations with the use of the instant explosion as the model of an energy deposition give only the qualitative understanding of the considered phenomenon. In addition, in the experiment the heated area is of a pulsing character in time which can be connected

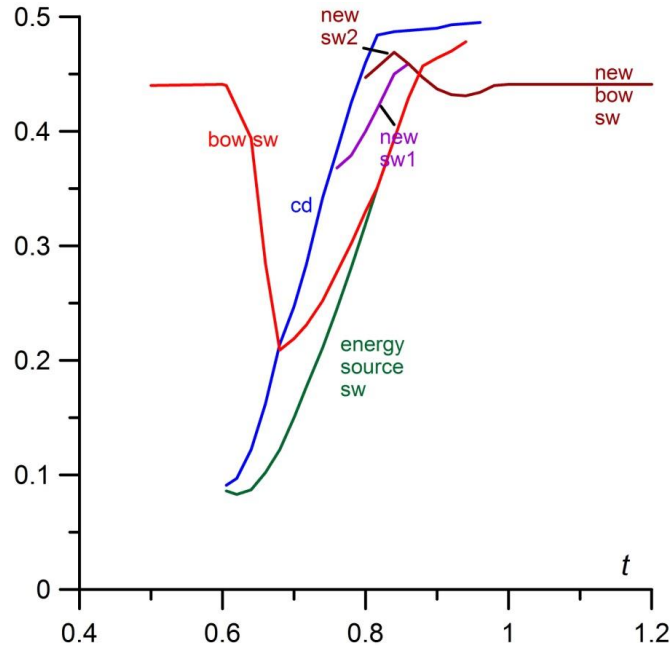


Figure 7: Dynamics of shock waves during energy source-shock layer interaction, $p_i=33.2$

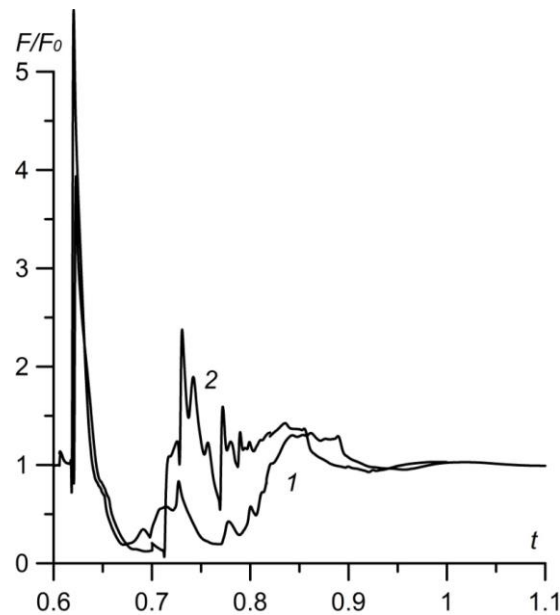


Figure 8: Dynamics of relative front surface drag force during energy source – shock layer interaction:
curve 1 - $p_i=33.2$; curve 2 - $p_i=19.4$ ($\eta=0.04$)

with complicated plasma processes needed to be described using non-aquilibrium approach. Also the time of the formation of the plasma area is not known in the experiment. Nevertheless, the qualitative features of the experimental results are in agreement with the conducted simulations:

- steady flow with the right shape and the close value of standoff of the bow shock wave (Fig. 3);
- generating three shock waves in the region between the left part of the source shock wave and the body at the initial and middle stages of the interaction (Fig. 2b vs flow image in Fig. 5 for $t=0.76$);
- generating a series of shock waves in the vicinity of the body at the middle stage of the interaction (Fig. 2c vs flow image in Fig. 5 for $t=0.8165$);
- forming a new strong shock wave near the body which moves from the body and passes through the left shock wave at the middle and final stages of the interaction (Fig. 2d, 2e vs flow images in Fig. 5 for $t=0.86-0.9$);
- formation of a new bow shock from this new shock wave which is accompanied by a pulsation of this new bow shock (during the new steady flow establishing at the final stage of the interaction) (Fig. 2d-2f vs flow images in Fig. 5 for $t=0.9-1.2$; see, also Fig. 7)

5. Summary

High speed shadow images have been obtained experimentally for the process of the impact of the plasma area (plasmoid) on the supersonic layer over AD body “blunt cone - cylinder” at Mach number 3. The images showed that the bow shock wave standoff on the axis of symmetry increases significantly – up to 4 cm. The moving of the bow shock wave from the body is accompanied by the front drag force decrease.

Numerical simulations on the base of the Euler system of equation with the use of the model of an energy deposition as an instant explosion in gas have been conducted. The simulations provided the qualitative understanding of the considered phenomenon and showed the sufficient agreement between the numerical flow patterns and the experimental images. In addition, the elements of arising shock wave structures have been obtained which coincided with the experimentally obtained ones. Study of the dynamics of stagnation pressure showed that for obtaining a continuous in time drag force reduction the significantly great pressure values should be achieved in the plasmoid.

The research is supported by RSF under the Project No 18-19-00672.

References

- [1] Knight, D. 2008. Survey of aerodynamic drag reduction at high speed by energy deposition. *J. Propuls. Power* 24(6):1153-1167.
- [2] Russel, A., Zare-Bentash, H., Kontis, K. 2016. Joule heating flow control methods for high-speed flows. *J. Electrostatics* 80:34-68.
- [3] Georgievsky, P.Y., Levin, V.A. 1988. Supersonic flow over bodies in the presence of external energy input. *Pis'ma Zhurnal Tekh. Fiziki* 14:684-687 (in Russian). Available online: <http://journals.ioffe.ru/articles/viewPDF/31216>
- [4] Riggins, D., Nelson, H. and Johnson, E.. 1999. Blunt-Body Wave Drag Reduction Using Focused Energy Deposition. *AIAA Journal*, 37(4): 460-467.
- [5] Kolesnichenko, Y.F., Brovkin, V.G., Azarova, O.A., Grudnitsky, V.G., Lashkov, V.A., Mashek, I.Ch. 2002. Microwave Energy release regimes for drag reduction in supersonic flows. *Paper AIAA-2002-0353*, 1-12.
- [6] Knight, D., Kolesnichenko, Y.F., Brovkin, V.G., Khmara, D., Lashkov, V.A., Mashek, I.Ch. 2009. Interaction of Microwave-Generated Plasma with a Hemisphere Cylinder at Mach 2.1. *AIAA Journal*. 47(12):2996-3010.
- [7] Knight, D., Kolesnichenko, Y.F., Brovkin, V.G., Khmara, D., Lashkov, V.A., Mashek, I.Ch. 2010. Interaction of Microwave-Generated Plasma with Hemisphere-Cone-Cylinder, Aerospace Sciences Meeting and Exhibit, AIAA, DOI 10.2514/6.2010-1005.
- [8] Azarova, O.A., Knight, D.D. 2015. Numerical Prediction of Dynamics of Microwave Filament Interaction with Supersonic Combined Cylinder Bodies, *AIAA*, DOI 10.2514/6.2015-0581.
- [9] Tretyakov, P.K., Fomin, V.M., Yakovlev, V.I. 1996. New principles of control of aerophysical processes – research development. In: *Proc. Int. Conference on the Methods of Aerophysical Research, Novosibirsk, Russia, 29 June - 3 July, 1996*. Novosibirsk: Inst. Theoretical and Applied Mech., part 2, pp. 210–220.
- [10] Adalgren, R.G., Yan, Hong, Elliott, G.S., Knight, D.D., Beutner, T.J., Zheltovodov, A.A. 2005. Control of Edney IV Interaction by Pulsed Laser Energy Deposition. *AIAA Journal*. 43(2):256-269.
- [11] A.A. Zheltovodov, E.A. Pimonov, D.D. Knight, Energy Deposition Influence on Supersonic Flow over Axisymmetric Bodies, *AIAA* (2007), DOI 10.2514/6.2007-1230.
- [12] Mortazavi, M., Knight, D., Azarova, O., Shi, J. and Yan, Hong. 2014. Numerical Simulation of Energy Deposition in a Supersonic Flow past a Hemisphere. *Paper AIAA-2014-0944*, 1–18.
- [13] Azarova, O.A., Knight, D.D. 2017. Interaction of microwave and laser discharge resulting “heat spots” with supersonic combined cylinder bodies. *Aerospace Science and Technology*. 43:343-349.
- [14] Lapushkina, T.A., Erofeev, A.V. 2017. Supersonic flow control via plasma, electric and magnetic impacts - *Aerospace Science and Technology*. 69: 313-320.
- [15] Znamenskaya, I.A., Naumov, D.S., Sysoev, N.N., Chernikov, V.A. 2019. Analysis of Dynamic Processes Occurring during Generation of Plasmoid Formations in a Supersonic Flow. *Technical Physics*, Vol. 64, No. 6, pp. 802–806. © Pleiades Publishing, Ltd..
- [16] Azarova, O.A. 2015. Complex conservative difference schemes for computing supersonic flows past simple aerodynamic forms, *Comp. Math. Math. Phys.* 55 (12): 2025-2049.